ISSN 2229-5518

A framework for palm tree detection from WorldView 2 imagery using contextual texture-based classification and local maxima filtering

Soufiane IDBRAM, Aissam Bekkari, Azeddine Elhassouny and Driss MAMMASS

Abstract— In this study, we present a hybrid framework for palm tree detection by combining two processes. In the first one, we apply a supervised contextual texture-based classification algorithm to a combined layer of pan-sharpened multi-spectral (MS) bands and texture measures. Texture is modeled with the joint distribution of the Local Binary Pattern (LBP) operator, local variance and NDVI ratio. The contextual classification method is based on Markov Random Fields. Palm tree objects and their shadow are derived from the classified image. The second process is based on a new local maxima filtering (LM) using watershed map to extract the plausibles treetops positions. The classification result provides additional information allowing by combining it with the LM result to correct/complete the palm tree objects identification.

The proposed method is evaluated on five subsets of a WorldView 2 high-resolution imagery of a date palm grove area on the southwest of Morocco, the experimental results show that the proposed method outperforms the standard LM filtering and the traditional classifiers (MLC and SVM), thus achieving higher detection accuracy.

Index Terms— Contextual classification, local binary pattern, local maxima filtering, palm tree detection, watershed segmentation, WorldView 2 imagery.

1 Introduction

Palm groves are one of the most characteristic agro-ecosystems of Morocco, not only for their natural and scenic value, but also because of the socio-economic impact. Therefore, conservation and monitoring have become a primary objective, thus, knowledge of spatial distribution of palm tree becomes a necessity.

In this sense, remote sensing presents an effective tool to map palm groves, to count palm trees, and to detect their possible diseases, several studies have extended methods developed for optical imageries to detect single trees. Those methods include many techniques (filtering, segmentation, classification etc.).

In the case of methods filtering techniques, Local maxima filtering (LM) [1], [2] and watershed segmentation [3], [4], [5] are commonly used for treetops detection and tree crown segmentation and are ready for operational application because of their rapid implementation while maintaining the capability to produce relatively accurate results [6].

For the classification techniques, classification process can be performed in several ways, e.g., supervised or unsupervised, parametric or nonparametric, contextual or non-contextual. In the category of contextual methods, probabilistic ones represent another branch of powerful tools in image classification [7]. In particular, stochastic models have evolved from Markov Random Fields (MRF) to object processes. The fundamental idea of the MRF is to introduce contextual relations on a local neighborhood. Thus, besides spectral values for each pixel, information from its neighboring pixels is also evaluated. Various stochastic models have been proposed to detect tree from remote sensing data [8], [9], [10]. However, the optimization process is typically lengthy and computationally expensive, thereby, several research work have opted for deterministic methods such as the Iterated Conditional Mode (ICM).

The usefulness of incorporation of texture measure for mapping tree species using high resolution MS imagery is well established [11]. More details of texture measures can be found in [12] and its application in remote sensing in [13]. Among texture operators, a relatively new and simple texture model is Local Binary Pattern (LBP) [14], [15]. It is a theoretically simple yet efficient multi-resolution approach to gray scale and rotation invariant texture classification.

This study presents a framework used to detect palm trees from remote sensing imagery following two levels of image processing techniques. In the first level, we focus on the application of a supervised contextual classification method using Markov Random Fields. In this regard, we have used the ICM algorithm developed in [16] [17] to model the *prior* distribution of the image as a locally dependent MRF, for which the maximum *a posteriori* estimate is approximated iteratively. As input variables for the classifier, a combined layer of pan-sharpened multi-spectral (MS) bands and texture measures were used. Texture is

- *Soufiane Idbraim is an assistant professor of computer science in the Faculty of Science, Ibn Zohr University, Agadir, Morocco. E-mail: s.idbraim@uiz.ac.ma*
- *Aissam Bekkari received a PhD degree in computer science from Ibn zohr University, Agadir, Morocco. E-mail: a_bekkari@yahoo.fr*
- *Azeddine Elhassouny is an assistant professor of computer science in ENSIAS, Mohammed V University, Rabat, Morocco. E-mail: info_ azeddine@yahoo.fr*
- *Driss Mammass is the director of the high school of Technology of Agadir, Ibn Zohr University, Agadir, Morocco. E-mail: d.mammass@uiz.ac.ma*

ISSN 2229-5518

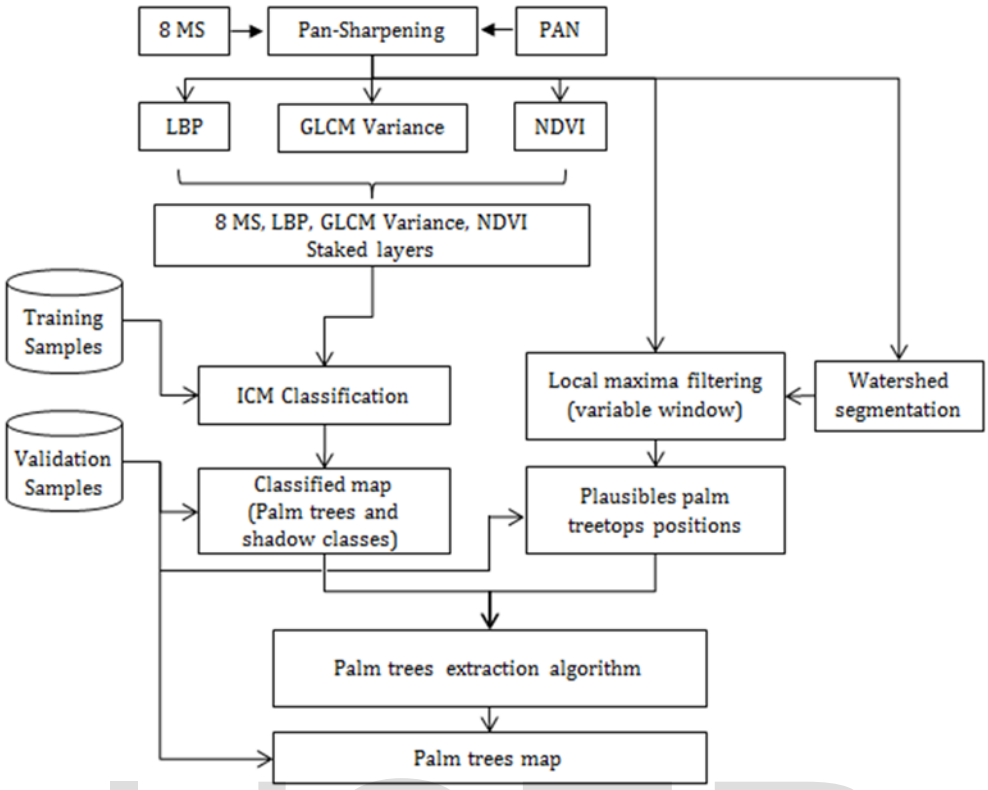

Fig. 1. Processing flow chart of the palm trees mapping.

modeled with the joint distribution of the Local Binary Pattern (LBP) operator, local variance and NDVI ratio. The second level is based on a new local maxima filtering using watershed map to extract the plausibles treetops positions, this result will be corrected and completed with that of the first level in a post-processing.

This paper is organized as follows. Section 2 is dedicated to the formulation of our proposed model. We provide an overview of the processing workflow, followed by detailing the model levels. Section 3 describes the study area, the data used in the study and the achieved results. Finally, conclusions are given in Section 4.

2 Methodology

2.1 The proposed workflow

Due to the complexity of the scenes and of the several factors limiting digital palm trees detection, our conceptual workflow incorporates a preprocessing step followed by two main blocks and finaly a post-processing step. The first block is devoted to the classification, the classified image is compared with the validation samples to determine the level of accuracy of the resulting classification. The second is related to the palm treetops detection, the detected palm trees are compared with the reference data. The post processing aims to combine the two results to identify correctely palm trees. The workflow outlining steps of our methodology is shown in Figure 1.

2.2 Preprocessing

The preprocessing starts with a process of fusion where the multispectral bands were resampled through the Gram-Smith Spectral sharpening with the panchromatic band. Thus, an image is obtained that has not only a higher spatial resolution, but also all the spectral information. Then to the pan-sharpened multi-spectral (MS) image we add three other texture bands of the joint distribution of the Local Binary Pattern (LBP) operator, local variance and NDVI ratio.

2.2.1 Review of local binary patterns

The local binary pattern (LBP) operator introduced by Ojala et al. [15] is a computationally efficient yet powerful means of texture description. It probes an image by comparing, for each pixel of the image, its gray value with each gray value of its neighboring pixels in a sequential, clockwise way. Then, the differences between the central pixel value and its neighboring values are encoded into a binary pattern. Formally,

$$\boldsymbol{LBP_{R,P}} = \sum_{P=0}^{P-1} \boldsymbol{u}(\boldsymbol{g_P} - \boldsymbol{g_c}).\boldsymbol{2^p}\,,\ \boldsymbol{u}(\boldsymbol{x}) = \begin{cases} \mathbf{1}, & \boldsymbol{x} \geq \mathbf{0} \\ \mathbf{0}, & \boldsymbol{x} < \mathbf{0} \end{cases} \quad (1)$$

where g_c is the gray value of the central pixel, g_p is the value of its pth neighbor, P is the total number of neighbors equally located on a circle of radius R. On this circle, if a neighbor position does not perfectly fit with the center of a

ISSN 2229-5518

pixel (as it often occurs, as shown in Figure 2) its gray value is calculated by using bi-linear interpolation. The resulting patterns are then accumulated into a histogram to represent statistically the texture content of an image.

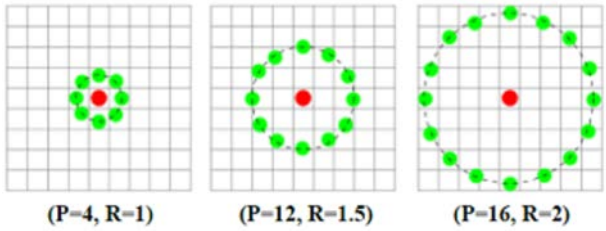

Fig. 2. Circularly symmetric neighbor sets for different (R,P) values of LBP.

The LBP approach has several desirable properties: gray-scale invariance, computational simplicity, and impressive discriminant power. However, the LBP operator produces fairly high dimensional feature vectors (2*P* distinct values). This high dimensionality makes it in practice intractable to be used by a classifier for a "large" (> 16) value of *P*. One solution is to only consider the "uniform" patterns [15]. The *U* value of LBP is defined as the number of spatial transitions (bitwise 0/1 changes):

$$U(LBP_{R,P}) \quad |u(g_{P-1}-g_c)-u(g_0-g_c)| + \sum_{P=1}^{P-1} |u(g_P-g_c)-u(g_{P-1}-g_c)| \tag{2}$$

The patterns which have an *U* value of at most 2 are defined as "uniform" patterns. Thus, the histogram dimension is reduced to $P(P-1)+3$.

Furthermore, the rotation invariant uniform LBP is achieved by the following formulas:

$$LBP_{R,P}^{riu2} = \begin{cases} \sum_{P=0}^{P-1} u(g_p - g_c), \text{ if } U(LBP_{R,P}) \le 2 \\ P+1, \qquad \text{otherwise} \end{cases} \tag{3}$$

Therefore, mapping from $LBP_{R,P}^{u2}$ to $LBP_{R,P}^{riu2}$ further reduces the length of the feature vector to $P+2$, leading to a more compact image representation.

2.2.2 GLCM variance

As cited previously, the approach of LBP hase a gray scale invariance property,thus, the classifier will be reinforced by the incorporation of another texture measure proposed by Haralick et al. [12] which is the Gray-Level Co-occurrence Matrices variance (GLCM variance) in average over all four different directions (0, 45, 90 and 135). Since texture has multi-scale perspective, the window size for texture synthesis plays an important role. Considering small patch size of palm tree in the study area, 3 × 3 window size was used.

$$GLCM\ var = \sigma_{i,j}^2 - \sum_{i,j=0}^{N-1} p_{i,j}(i,j-\mu_{i,j}) \tag{4}$$

i is the row number, *j* is the column number; $p_{i,j}$ is the normalized frequencies at which two neighboring pixels separated by a constant shift occur in the image, *N* is the dimension of the GLCM, i.e., the number of grey levels present in the image.

2.2.3 NDVI

It is beneficial to mask vegetation in the PAN-MS image in order to reduce computational load and confusion. So, the Normalized Difference Vegetation Index (NDVI) [18] definded in (5) is used as a sensitive indicator to mask out everything that is not vegetation.

$$NDVI = \frac{NIR-RED}{NIR+RED} \tag{5}$$

where *NIR* is the reflectance value of the near-infrared channel (band 7), and *RED* is the reflectance value of the red channel (band 5). Vegetation has a high reflectance in the *NIR* channel and a low reflectance in the *RED* channel. Consequently, the NDVI equation produces values in range of -1.0 to 1.0, where increasing positive values indicate increasing green vegetation and negative values indicate non vegetated surface features.

2.3 ICM classification

2.3.1 MRF in imagery

We are given an image *MxN* defined on $\Omega = \{s=(i,j); 1 \le i \le M, 1 \le j \le N\}$ with value in E, thus, an element x_s of *E* is a matrix $x = (x_s, s \in \Omega)$ where x_s is for example the gray scale associated to the site *s*.

To the family $V = \{V(s), s \in \Omega\}$ is associated a class of the distribution probability, called Markov field and characterized by the following property:

$$\begin{cases} P(x_x) \succ 0, & \text{for any configuration } x_s \\ P(x_s | x_r, r \in \Omega - \{s\}) = P(x_s | x_r, r \in V(s) - \{s\}) \end{cases} \tag{6}$$

The probability of a pixel x_s conditional to all the others is equal to the conditional probability of x_s knowing the pixels of its local neighborhood *V(s)*. The value of the other sites *r* is supposed known $r \in \Omega - \{s\}$. In the context of land cover classification, this property implies that the same land cover class is more likely to occur in connected regions than isolated pixels.

The theorem of Hammersley-Clifford [19] makes it possible to characterize the MRFs in overall terms from the expression of the *a priori* probability of a configuration of the classes $P(X=x)$. It allows to establish a correspondence between a Markov field and a Gibbs field when no realization of *X* has a null probability. It shows that a definite random field on a network is a Markovian field if and only if its distribution of the *a priori* probability *P(x)* is a Gibbs distribution, defined by:

$$P(x) = \frac{1}{Z} e^{-U(x)} \tag{7}$$

where Z is a normalizing constant.

2.3.2 The estimation criteria in MRF

There are several criteria for estimating the variables of

ISSN 2229-5518

interest x, the one which is applied is the estimator of the Maximisation of the *a posteriori* (MAP), so that the best estimate is the most probable given the observed realization y and which amounts to minimize energy $U(x)$.

In the case of MAP, there exist several methods of researching its solution: deterministic or stochastic. In our work we have opted for a deterministic method, which is the Iterated Conditional Mode method (ICM), because the convergence is guaranteed with a reasonable time of execution.

2.3.3 Minimization of the posterior energy by the ICM

Proposed by Besag [19], by assigning to each site s the class that maximizes the conditional probability to the observation in s and therefore minimizes the function of energy.

Let $Y = \{Y_s = y_s ; s \in \Omega\}$ and $X = \{X_s = x_s ; s \in \Omega\}$. Each pixel configuration x_s denotes one land cover class. Hence, $x_s \in \{1,..., L\}$. A simple way to see this method is using Markovian property as follows: developing the *a posteriori* probability compared to a pixel s, we choose as a new value in s the one that maximizes the conditional probability $P(X = x|Y = y)$, which can be written as,

$$X^* = \arg\left\{\max_X \left[P(y|x = x_s)P(x_s)\right]\right\} \tag{8}$$

here, $P(y|x = x_s)$ is the probability that the data point y is observed for the given class of the configuration x in the site s, whereas $P(x_s)$ denotes the *a priori* probability of the configuration x_s. To calculate the probability $P(y|x = x_s)$, a multivariate Gaussian distribution with mean vector μ_s and covariance matrix $\sum_s$ is assumed for class in x_s :

$$P(y|x = x_s) = \frac{1}{(2\pi)^{d/2}|\Sigma_s|^{1/2}} \times \exp\left[-\frac{1}{2}(y_s - \mu_s)^T \Sigma_s^{-1}(y_s - \mu_s)\right] \tag{9}$$

where d is the number of spectral bands.

The common covariance matrix is $\Sigma = \frac{1}{L}\sum_{i=1}^{L}\Sigma_i$.

Substituting (9) into (8), yields,

$$X^* = \arg\left\{\max_X \left[C\exp(-E(X|Y))\right]\right\} \tag{10}$$

where $C = 1/Z_T(2\pi)^{d/2}$ and

$$E(X|Y) = \frac{1}{T} \times U(x_s) + \frac{1}{2}(y_s - \mu_s)^T \Sigma_s^{-1}(y_s - \mu_s) + \frac{1}{2}\ln(|\Sigma_s|)$$

Since the exponential function is monotonic and C is a constant that is independent of X, (10) can be reduced to:

$$X^* = \arg\left\{\min_X \left[E(X|Y)\right]\right\} \tag{11}$$

2.3.4 ICM method with contextual constraints

The formalism of Markov Random Fields makes it possible to introduce, in a flexible way, the constraints of spatial context through their modeling by some potential functions. We have used the method developped in [17], in addition to the constraint of the neighbourhood (regularization or smoothing constraint) the method introduced another constraint which is that of the contour (segmentation) in order to minimize more the function of energy (11) in the classification. The expression of the function of energy, corresponding to the constraints used in the modeling of the *a priori* probability is as follow:

$$E(X|Y) \propto \frac{1}{T}U(x_s) + f(y_s, \mu_s, \Sigma_s) \tag{12}$$

where

$$U(x_s) = \sum_{all\_constraints} U_{constraints} = U_{smooth}(x_s) + U_{contour}(x_s) \tag{13}$$

for more details refer to [17].

2.4 Local maxima filtering

2.4.1 Segmentation map

In this step we begin with the realization of the segmentation map, thus, we extract closed and squelettized contour from the image of powers contours known as the gradient image produced by a Shen-Castan filtering. The program will perform a watershed algorithm [17] with a simple threshold. It is a method resulting from the mathematical morphology, systematic and effective to provide directly squelettized and closed contours. If we consider the image of powers contours as a surface in the 3D space, we can use the terminology of geography which defines the watershed as the limit between two catchment basins. The method consists in simulating a filling of the basins of the image of powers contours beginning with the local minima, until the meeting of water of the neighbouring basins which forms the watershed. At this place, we construct a dam to announce the presence of a contour. The threshold of segmentation causes to fill the basins until a height equal to the threshold without constructing the dams (hence the contours), then we repeat the usual process. For a threshold of zero, we find the classical watershed algorithm.

The implemented program allows a maximum of 256 levels of immersion, which means 256 possible thresholds segmentation (0-255).

As the shape of palm tree is circular or elliptical, the choice of threshold is based on a shape index. Segment shape is obtained by calculating segment length/width proportion and a shape index defined as:

$$S = \frac{e}{4\sqrt{A}} \tag{14}$$

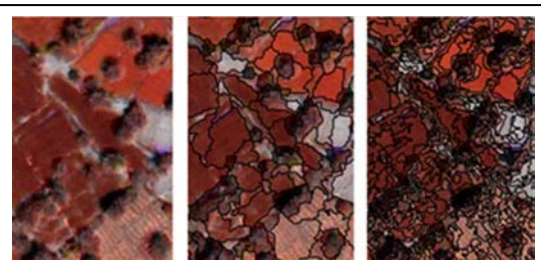

Fig. 3. Watershed segmentation thresholding.

The shape index S is the border length e of the image segment divided by four times the square root of its area A.

ISSN 2229-5518

2.4.2 Variable window LM filtering

To optimize the performance of local maximum filtering, we first smoothed the pan-sharpened multi-spectral (PAM-MS) image using Gaussian smoothing, this filtering method uses a bell-shaped Gaussian distribution. Thus, the filter reduces the noise level in the image and also raises the radiometric values of the palm tree peaks, which theoretically results in reduced overestimation errors. Smoothing based on a Gaussian core is driven by two parameters, namely the standard deviation and window size. In this study, standard deviation σ and window size were set to 1 and 3 × 3 pixels.

Wulder et al. [2] have showed that the success of local maximum filtering in locating trees depends on the size and distribution of trees in relation to the image spatial resolution. A static-sized 3x3 pixel LM filter provides an indication of the maximum number of palm trees that may be found in the imagery, yet high errors of commission reduce the integrity of the results. They have demonstrated that the variable window-size techniques allow a reduction in both the errors of commission and omission. From this finding, we propose a new concept of variable windowing, it is based on the watershed segmentation map. In the search for maxima, we consider for each pixel the corresponding segment that contains it, or in the case where the pixel is on the contour, we consider the largest segment of those they share it. At the end of this stage we will have a map of plausibles palm treetops positions.

2.5 Post-processing

In this step we select the accurate configuration of palm treetops by combining the classification and LM filtering results according to the proposed algorithm.

Let PTT denote the palm treetops and C_P denotes the Palm tree class

$\boldsymbol{for}$ $each\ PTT_i$

  $\boldsymbol{if}$ $PTT_i \cap C_P$ $\boldsymbol{then}$

    we keep this PTT_i

  $\boldsymbol{else\ if}$ $\exists\ C_{P_{1\ldots j}} \epsilon\ 7x7\ PTT_i\ neighborhood$ $\boldsymbol{then}$

    we take the center of $[PTT_i\ ,\ CG(C_{P_{1\ldots j}})]$ as a new $PTT_{i'}$ instead of PTT_i

  $\boldsymbol{else}$

    we decline PTT_i

  $\boldsymbol{end\ if}$

$\boldsymbol{end\ if}$

$\boldsymbol{end\ for}$

---

where CG is the center of gravity of the segment and j is equal at least to 5 pixels which is equivalent to 1.25 m² of palm tree surface.

3 Result and Discussion

3.1 Study area

The study area is the date palm grove of Mezguita (Figure 4), in the Draa River Valley, Morocco. It has an extension of 44 km². The mean altitude is near 900 m above sea level. The area is characterized by a prevalence of small property. 85.8 % of farms have a surface lower than 2 ha and only 5.3 % of farms have a surface higher than 5 ha. In this very fragmented zone where date palms coexist with other crops.

3.2 Satellite data

A 9 km x 4.9 km Worldview-2 (WV2) image of the Mezguita Oasis (Figure 4), acquired on 25 July 2013 was used. The acquisition was slightly off-nadir at 83.2° satellite elevation. The image was supplied at the nominal spatial resolution of 0.50 m/pixel and 2 m/pixel for the panchromatic and multispectral bands, respectively.

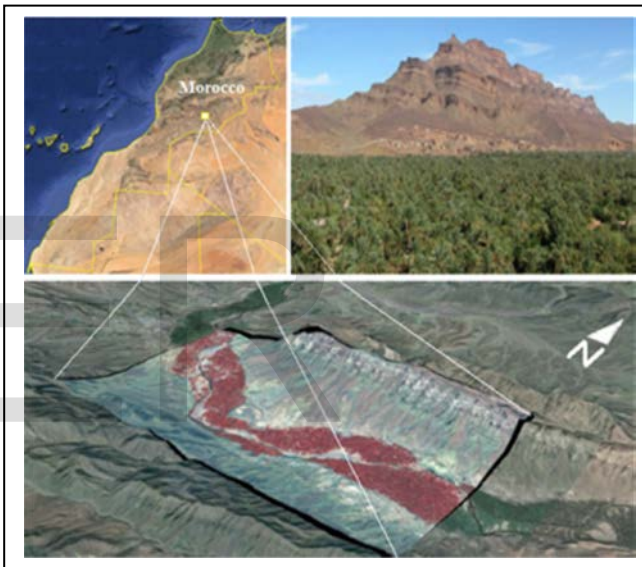

Fig. 4. Worldview-2 image of the Mezguita Oasis.

From the satellite imagery, we have created five subsets of 200 x 200 m which presents scenes with differents degrees of overlap.

3.3 Classification result

To evaluate the classification results, we have also made some tests with the most used non-contextual classifier namely ML and SVM using ENVI Software. The comparison between these two categories shows the contribution of the contextual classification (Table 1). The ICM classification results are represented in the Figure 5. We observe the interest of the use of texture with the joint distribution of the Local Binary Pattern (LBP) operator, local variance and NDVI ratio information to refine the result, the red rectangle shows an example of misclassification of the palm tree class.

ISSN 2229-5518

Table 1 shows a summary of overall percentage accuracy results, we note that the non-contextual results (ML and SVM) did not allow good palm trees class detection (75.7% and 81.2% respectively of total accuracy using ENVI Software). On the contrary, for the ICM method a total palm trees accuracy of 84.8 % was achieved. This percentage increases with the use of the selected texture features to reach a total accuracy of 91.5%.

TABLE 1
PALM TREES CLASSIFICATION ACCURACY

	User's accuracy	*Producer's accuracy*
ML	75,2 %	76,1 %
SVM	80,8 %	81,5 %
ICM	85,3 %	84,2 %
ICM+Texture	92,3 %	90,7 %

3.4 Local maxima filtering result

The figure 6 presents the comparaison between a standard static-sized LM filtering and our proposed variable window LM filtering based on watershed segmentation map. For the classical method we have chosen a window size of 3x3 according to [2]. From a visual results interpretation we notice the big difference between the two results, we can say that standard LM may give us an idea about the number of palm trees but does not detect them exactly, contrary to our method which enables us to distinguish better the treetops. However, there are some false detections that can be corrected through the next step.

To evaluate the performances of the proposed LM filtering, the detected palm trees are compared with the reference data (500 palm trees from the 5 subsets). The comparison results of the entire aggregated palm trees from the detected palm trees and the reference data can be classified into the following three categories: the correctly detected palm trees (correct), palm trees in the detection results that have no corresponding reference palm tree (commission) and palm trees in the reference data not detected (omission). Commission/Omission statistics and the overall detection accuracy are used to quantify the detection results. Table 2 shows a summary of overall percentage accuracy results. The overall accuracy of palm trees detection based on the LM filtering using segmentation map exhibited a largely higher accuracy (77.01%) than that with a standard LM filtering (53.6%).

3.5 Post-processing result

In this step we select the plausibles palm treetops by combining the classification and LM filtering results according to the proposed algorithm (section 2.5). The figure 7 illustrates this result.

It is interesting to note from figure 7 that the aim when applying the proposed algorithm is to maintain the number of legitimate palm trees found while also minimizing the amount of pixels falsely identified as palm treetops, thus, additional palm tree detection errors may not arise in this step. The overall accuracy of palm tree detection reached 92.2%.

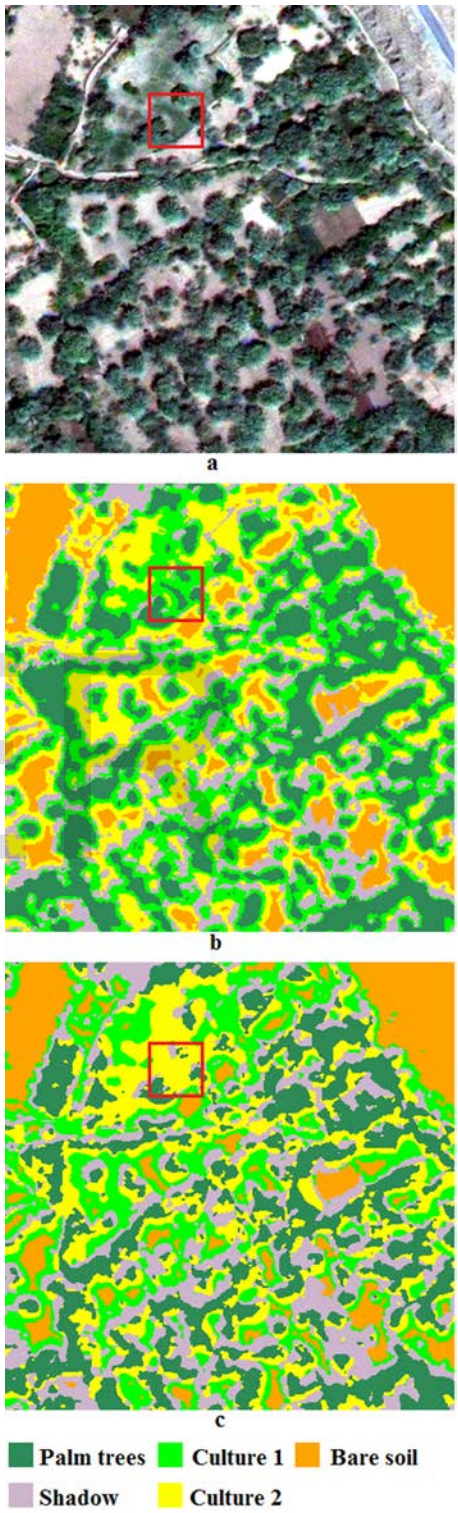

Fig. 5. a- [5,3,2] bands color composite. b- ICM classified map. c- ICM with texture classified map.

TABLE 2
RESULTS OF THE PROPOSED FRAMEWORK COMPARED WITH LM FILTERING AND LM FILTERING WITH SEGMENTATION MAP (REFERENCE DATA : 500 PALM TREES)

	Detected palm trees	Correct		Commission		Omission		Overall accuracy (%)
		No.	%	No.	%	No.	%	
Standard LM filtering	612	388	63.4	224	36.6	112	22.4	53.6
LM filtering with segmentation	578	469	81.14	109	18.86	31	6.2	77.01
Post-processing	461	461	100	0	0	39	8	92.2

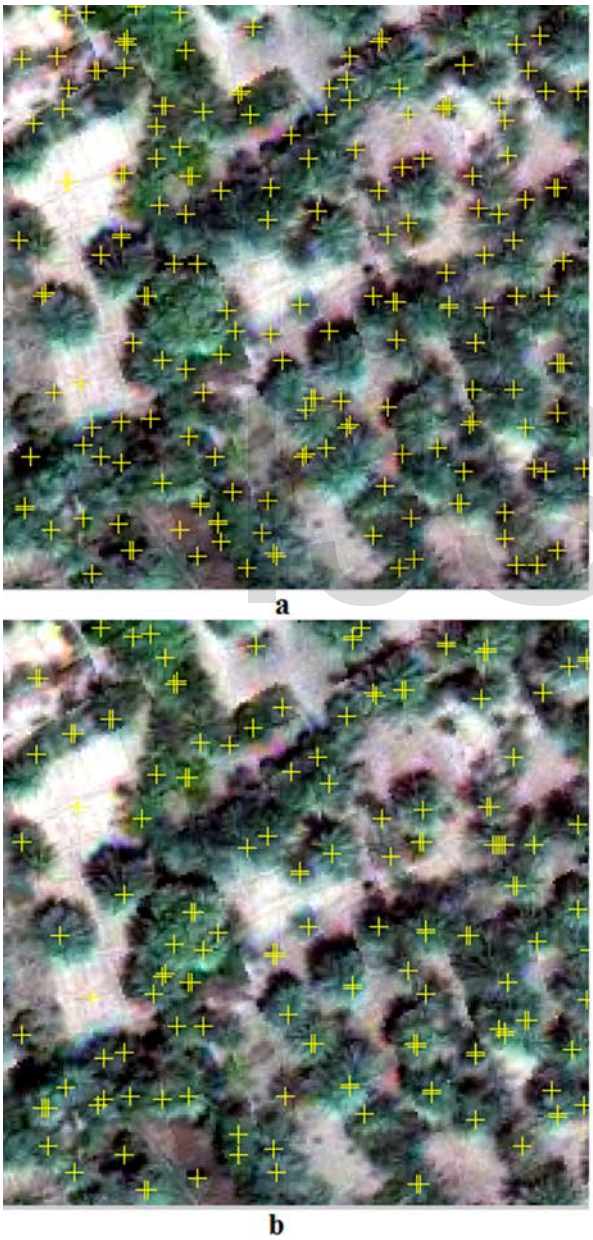

Fig. 6. Palm treetops from : a- 3x3 LM filtering. b- the proposed variable window LM filtering.

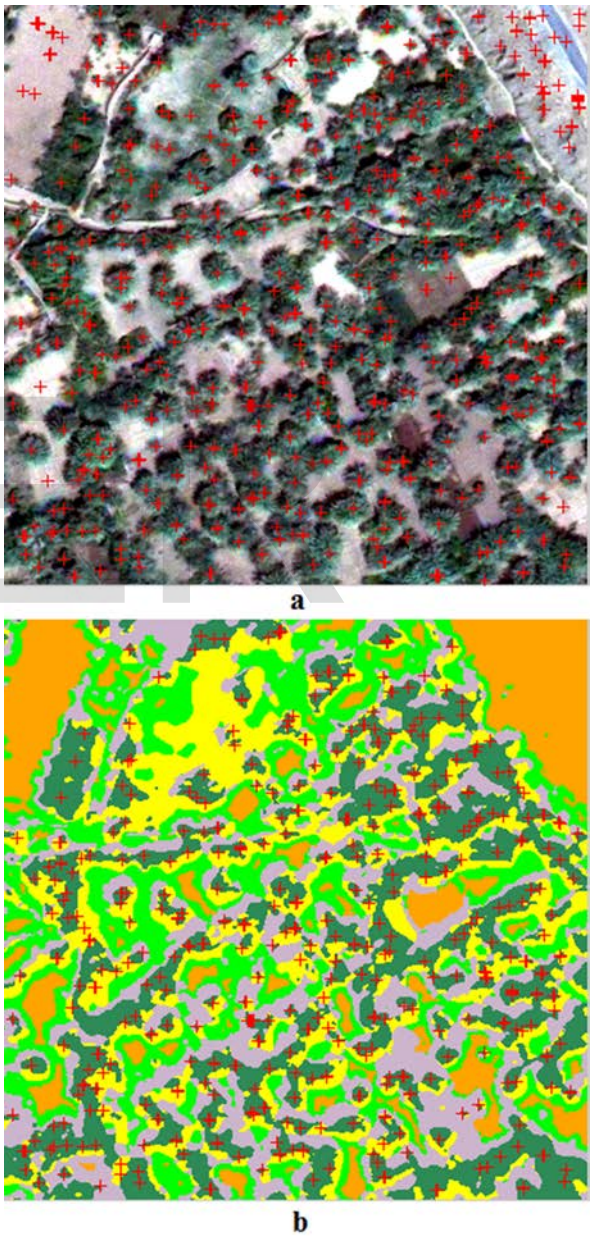

Fig. 7. a- palm treetops from the proposed variable window LM filtering. b- retained palm treetops after the execution of the algorithm.

4 Conclusion

In this paper we have proposed a framework to detect single palm trees from WordView 2 satellite imagery by combining the image processing techniques of LM filtering and ICM classification. The local maxima filtering based on a watershed segmentation map, worked remarkably well for the detection of palm treetops compared to a standard LM. Moreover, the comparative analysis between classifiers demonstrates that the proposed ICM classifier with the joint distribution of the Local Binary Pattern (LBP) operator, local variance and NDVI ratio outperforms ML, SVM and ICM. Through a proposed algorithm, the two results will complete each other, to develop the final palm trees map.

The significance of this study is that the present framework is capable of accurately identifying palm trees as well as detecting other tree species, however, the case of overlapping still significant issue for further investigation.

Acknowledgment

Satellite imagery and ground truth data of this work are provided in the PALMERA project 2008-2013 included in the POCTEFEX program financed by the FEDER

References

[1] S.C. Popescu, R.H. Wynne and R.F. Nelson, "Estimating plot-level tree heights with lidar: local filtering with a canopy-height based variable window size," *Comput. Electron. Agr.*, 37, pp. 71–95. 2002.

[2] M. Wulder, K.O. Niemann and D.G. Goodenough, "Local maximum filtering for the extraction of tree locations and basal area from high spatial resolution imagery," *Remote Sens. Environ.*, 73, pp. 103–114, 2000.

[3] Q. Chen, D. Baldocchi, P. Gong and M. Kelly, "Isolating individual trees in a savanna woodland using small footprint lidar data," *Photogrammetric Eng. Remote Sens.*, 72, pp. 923–932, 2006.

[4] U. Pyysalo and H. Hyyppa, "Reconstructing tree crowns from laser scanner data for feature extraction," *Int. Arch. Photogrammetry Remote Sens. Spatial Inf. Sci.*, 34, pp. 218–221, 2002.

[5] L. Wang, P. Gong and G.S. Biging, "Individual tree-crown delineation and treetop detection in high-spatial-resolution aerial imagery," *Photogrammetric Eng. Remote Sens.*, 70, pp. 351–358, 2004.

[6] H. Kaartinen, J. Hyyppä, X. Yu, M. Vastaranta, H. Hyyppä, A. Kukko, M. Holopainen, C. Heipke, M. Hirschmugl, F. Morsdorf, E. Næsset, J. Pitkänen, S. Popescu, S. Solberg, B.M. Wolf and J.C. Wu, "An international comparison of individual tree detection and extraction using airborne laser scanning," *Remote Sens.*, 4, pp. 950–974, 2012.

[7] X. Descombes and J. Zerubia, "Marked point process in image analysis," *IEEE Signal Process. Mag.*, 19, pp. 77–84, 2002.

[8] X. Descombes and E. Pechersky, "Tree Crown Extraction Using a Three State Markov Random Field," Research Report RR-5982, INRIA, pp. 14, 2006.

[9] G.Perrin, X. Descombes and J. Zerubia, "A non-Bayesian model for tree crown extraction using marked point processes," Research Report RR-5846, INRIA, pp. 34, 2006.

[10] J. Zhang, G. Sohn and M. Brédif, "A hybrid framework for single tree detection from airborne laser scanning data: A case study in temperate mature coniferous forests in Ontario, Canada," *ISPRS J. Photogrammetry Remote Sens.*, 98, pp. 44–57, 2014.

[11] S.E. Franklin, R.J. Hall, L.M. Moskal, A.J. Maudie and M.B. Lavigne, "Incor-porating texture into classification of forest species composition fromairborne multispectral images," *Int. J. of Remote Sens.*, vol. 21, no. 1, pp. 61–79, 2000.

[12] R.M Haralick, K. Shanmugam and I. Dinstein, "Textural features for image classification," *IEEE Transactions on Systems, Man and Cybernetics*, vol. 3, no. 6, pp. 610–621, 1973.

[13] M.H. Batista and V. Haertel, "On the classification of remote sensing high spatial resolution image data," *Int. J. of Remote Sens.*, vol. 31, no. 20, pp. 5533–5548, 2010.

[14] M. Pietikäinen, T. Ojala and Z. Xu, "Rotation-invariant texture classification using feature distributions," *Pattern Recognition*, 33, pp. 43-52, 2000.

[15] T. Ojala, M. Pietikäinen, and T. Mäenpää, "Multiresolution gray-scale and rotation invariant texture classification with local binary patterns," *IEEE Transactions on Pattern Analysis and Machine Intelligence*, vol. 24, no. 7, pp. 971-987, 2002.

[16] A. H. S. Solberg, T. Taxt and A. K. Jain, "A Markov randomeld model for classification of multisource satellite imagery," *IEEE Trans. Geosc. Remo. Sens.*, 34, pp. 100-113, 1996.

[17] S. Idbraim, D. Ducrot, D. Mammass and D. Aboutajdine, "An unsupervised classification using a novel ICM method with constraints for land cover mapping from remote sensing imagery," *International Review on Computers and Software*, 4, pp. 165-176, 2009.

[18] J.W. Rouse, R.H. Haas, J.A. Scheel and D.W. Deering, "Monitoring Vegetation Systems in the Great Plains with ERTS," *Proc. 3rd Earth Resource Technology Satellite (ERTS) Symposium*, pp. 48-62, 1974.

[19] J. Besag, "Spatial interaction and the statistical analysis of lattice systems," *Journal of the Royal Statistical Society*, Series B, vol. 36, pp. 192-236, 1974.